Biochimica et Biophysica Acta 1837 (2014) 1350–1361

Contents lists available at ScienceDirect

Biochimica et Biophysica Acta

journal homepage: www.elsevier.com/locate/bbabio

Formation of highly organized intracellular structure and energy metabolism in cardiac muscle cells during postnatal development of rat heart

Tiia Anmann [a,*,1], Minna Varikmaa [a,b,1], Natalja Timohhina [a], Kersti Tepp [a], Igor Shevchuk [a], Vladimir Chekulayev [a], Valdur Saks [a,c], Tuuli Kaambre [a,d]

[a] Laboratory of Bioenergetics, National Institute of Chemical Physics and Biophysics, Tallinn, Estonia
[b] Faculty of Science, Department of Chemistry, Tallinn University of Technology, Tallinn, Estonia
[c] Laboratory of Fundamental and Applied Bioenergetics, Joseph Fourier University, Grenoble, France
[d] Institute of Mathematics and Natural Sciences, Tallinn University, Tallinn, Estonia

ARTICLE INFO

Article history:
Received 7 June 2013
Received in revised form 25 March 2014
Accepted 27 March 2014
Available online 3 April 2014

Keywords:
Mitochondria
Bioenergetics
Cardiomyocyte
Development
Tubulin
Intracellular architecture

ABSTRACT

Adult cardiomyocytes have highly organized intracellular structure and energy metabolism whose formation during postnatal development is still largely unclear. Our previous results together with the data from the literature suggest that cytoskeletal proteins, particularly βII-tubulin, are involved in the formation of complexes between mitochondria and energy consumption sites. The aim of this study was to examine the arrangement of intracellular architecture parallel to the alterations in regulation of mitochondrial respiration in rat cardiomyocytes during postnatal development, from 1 day to 6 months.

Respirometric measurements were performed to study the developmental alterations of mitochondrial function. Changes in the mitochondrial arrangement and cytoarchitecture of βII- and αIV-tubulin were examined by confocal microscopy.

Our results show that functional maturation of oxidative phosphorylation in mitochondria is completed much earlier than efficient feedback regulation is established between mitochondria and ATPases via creatine kinase system. These changes are accompanied by significant remodeling of regular intermyofibrillar mitochondrial arrays aligned along the bundles of βII-tubulin. Additionally, we demonstrate that formation of regular arrangement of mitochondria is not sufficient per se to provide adult-like efficiency in metabolic feed-back regulation, but organized tubulin networks and reduction in mitochondrial outer membrane permeability for ADP are necessary as well. In conclusion, cardiomyocytes in rat heart become mature on the level of intracellular architecture and energy metabolism at the age of 3 months.

1. Introduction

Adult cardiac cells display highly organized intracellular structure and energy metabolism [1]. Mitochondria are arranged in "crystal-like" order between myofibrillar lattice [2,3] and form close structural and functional contacts with the major ATP consumption sites in cytosol, e.g. myofibrils, sarcoplasmic reticulum and sarcolemma [4–6]. These tightly coupled complexes of mitochondria and ATPases are known as intracellular energy units (ICEU) and represent the basic organization pattern of energy metabolism in cardiomyocytes [4,5,7]. Metabolic feedback within ICEU is realized via phosphoryl transfer pathways, e.g. creatine kinase (CK), adenylate kinase (AK), direct ATP/ADP channeling [4–6,8,9]. The major phosphoryl carrier between mitochondria and ATPases in cardiomyocytes is creatine (Cr), which is channeling energy between compartmentalized isoenzymes of cytosolic CK (MM-CK) and mitochondrial CK (MtCK) [10]. Several previous studies have evidenced that the arrangement of mitochondria is crucial in regulation of MOM permeability for adenine nucleotides [11,12]. For example, myofibrillar disorganization, looser packing of mitochondria with myofibrils and SR in the muscle LIM (MLP)-null mouse heart evidenced increased accessibility of exogenous ADP to mitochondria with nearly 1.3 fold increase in the affinity of mitochondrial respiration for ADP (K^{app}_mADP) in soleus and cardiac fibers [13]. Similarly impaired direct mitochondrial energy channeling was also observed in hearts

Abbreviations: ANT, adenine nucleotide translocator; CK, creatine kinase; FFA, free fatty acids; ICEU, intracellular energetic unit; IMS, intermembrane space; K^{app}_mADP, apparent K_m of mitochondrial respiration for exogenous ADP; MI, mitochondrial interactosome; MOM, mitochondrial outer membrane; MtCK, mitochondrial creatine kinase; OXPHOS, oxidative phosphorylation; PK, pyruvate kinase; RCI, respiratory control index; VDAC, voltage-dependent anion channel; V_0, basal respiration rate; V_{max}, maximal ADP-stimulated respiration rate

* Corresponding author at: Laboratory of Bioenergetics, National Institute of Chemical Physics and Biophysics, Akadeemia tee 23, 12618 Tallinn, Estonia.
E-mail address: tiia.anmann@kbfi.ee (T. Anmann).

[1] The first two authors have contributed equally to the manuscript.

http://dx.doi.org/10.1016/j.bbabio.2014.03.015
0005-2728/

lacking the cytoskeletal protein desmin. Therefore, perturbation of cardiac cytoarchitecture may impair direct energy transfer between mitochondria and SR [13].

Also, studies with HL-1 cells (i.e. atrial cardiomyocyte tumor lineage) demonstrate that less organized intracellular structure and mitochondrial distribution entail marked increase in the value of apparent K_m for mitochondrial respiration ($K^{app}{}_m$ADP = ~50 μM), in contrast to 7-fold higher value in adult isolated cardiomyocytes (~360 μM) [12].

It has been proposed that high $K^{app}{}_m$ADP in adult isolated cardiomyocytes is a result of crowded intracellular environment. However, the notion that the low affinity of mitochondrial respiration for ADP is a cell type specific phenomenon, that is characteristic to highly oxidative tissues, strongly argues against this assumption and indicates that some specific cytosolic protein is involved instead. Due to the presence of mitochondrial–cytoskeleton interactions in intact permeabilized cardiac cells, the apparent K_m for exogenous ADP in regulation of mitochondrial respiration $K^{app}{}_m$ADP is over 10 folds higher in permeabilized cardiac cell ($K^{app}{}_m$ADP = 360 μM) than in isolated cardiac mitochondria ($K^{app}{}_m$ADP = 18 μM), where these interactions are lost during isolation of mitochondria [12,14]. Similarly, the apparent $K^{app}{}_m$ADP is decreased several folds when interactions between mitochondria and cytoskeleton are disrupted by mild trypsin treatment [11,15]. In addition, these studies have shown that if MOM is more readily permeable to ADP (i.e. isolated mitochondria, trypsin treated cardiac cells), then Cr is unable to maintain maximal respiration rate in the presence of pyruvate kinase and phosphoenolpyruvate system (PK/PEP) and almost 50% decline in respiration rate is observed [15,16]. Thus, limited permeability of MOM for ADP appears to be necessary for enhancing coupling between MtCK reaction and oxidative phosphorylation (OXPHOS) and serves to maintain constant cycling of ATP/ADP within mitochondria [10]. It is proposed, that regulation of the mitochondrial respiration by Cr is accomplished via cooperatively functioning proteins, i.e. ATP synthasome, MtCK, voltage dependent anion channel (VDAC) and tubulin that form a supercomplex called Mitochondrial Interactosome (MI) [8,10]. This supercomplex represents a key site for the control of mitochondrial respiration in adult cardiac cells [10,16].

We and others have previously found that mitochondrial functioning in cardiomyocytes are significantly influenced by the organization of cytoskeletal network that directs and anchors mitochondria to their subcellular target sites [4,11,12,17]. Furthermore, recent experimental data suggest that apart from their role in positioning mitochondria, cytoskeletal protein tubulin may also directly participate in regulation of mitochondrial functional behavior by binding to VDAC and restricting its permeability to adenine nucleotides [18,19]. Notably, tubulin is present in mitochondria isolated from a variety of cancerous and non-cancerous cell types and associates, as shown by immunoprecipitation, with VDAC [20]. Moreover, recent in vitro electrophysiological experiments with VDAC have shown that nanomolar concentrations of heterodimeric tubulin evoke partial closure of a channel [19]. This discovery has received further proof in reconstitution experiments with isolated brain and heart mitochondria where nearly 30 fold rise in the value of $K^{app}{}_m$ADP (from 11 ± 2 μM up to 330 ± 47 μM) was registered upon addition of 1 μM tubulin by respirometry [19,21]. In addition, increase in the content of free tubulin in cancer cells, by treatment with microtubule destabilizing agents such as colchicine and nocodazole, was found to result in depression of mitochondrial membrane potential, indicating that augmented levels of free tubulin may hamper metabolite exchange between mitochondria and cytosol [22]. Finally, recent immunocytochemical studies assessing the distribution of β-tubulin isoforms in adult cardiomyocytes identified βII-tubulin isoform localization in the vicinity of mitochondria suggesting that this isoform may be responsible for restricted permeability of MOM for ADP in cardiomyocytes [21,23,24]. Although the functional significance of βII-tubulin has been dissected somewhat in neurons, where it constitutes nearly 58% of total β-tubulin pool and is important for neurite formation and polarized organization of neurons, its role in cardiomyocytes is still totally unknown [25,26]. Therefore, further data is needed to verify if it is involved in mitochondrial respiration regulation and contribution to the establishment of diffusion restrictions for adenine nucleotides during cardiac development.

In contrast to adult, neonatal cardiomyocytes have significantly less organized intracellular architecture and more glycolytic metabolic profile [27–29]. The neonatal heart utilizes glucose as main energy substrate and shifts rapidly after birth toward OXPHOS with free fatty acids (FFA) becoming the predominant source of energy. The role of glycolysis decreases parallel with the fine-tuning of OXPHOS capacity and by the time the heart reaches its full maturation nearly 90% of total cellular energy needs are covered by OXPHOS [29]. Reliance on glycolysis during early developmental stages stems mainly not only from lower energy demands, greater anaerobic glycolytic capacity and higher glycogen reserves of the developing heart but also from lower availability of oxygen [27,29,30]. Thus, cardiac metabolism changes in response to oxygen and substrate availability during development. Although the activities of different isoforms of glycolytic enzymes are altering during postnatal development, such as lactate dehydrogenase isoforms (LDH1, LDH2, LDH4 and LDH4), the total activity of the LDH remains the same. This shift in isoenzyme activity reflects the change from anaerobic to aerobic metabolism during maturation [31]. Since sufficient data is available in the literature about glycolysis during postnatal development it was not further dissected in the current study [29,30,32,33].

Continuous developmental maturation of energy metabolism occurs in the growing heart to meet increasing functional and metabolic demands. This remodeling is shaped by various extracellular signals such as hormones, Ca^{2+} gradients and other extracellular signals [34–36]. For example, cardiomyocytes downregulate many regulatory and cytoskeletal components involved in cytokinesis after birth to uncouple cytokinesis from karyokinesis in cardiomyocytes and to cause binucleation of cardiomyocyte [37].

Previous studies have established that diffusion barriers for ADP are formed gradually during the first 6 postnatal weeks, as evidenced by the continuous rise in the value of $K^{app}{}_m$ADP [28]. Concurrently with the appearance of diffusion restrictions at the outer mitochondrial membrane maturation of the phosphotransfer system occurs. During the early embryonic stage MtCK expression is absent [38,39], but appears in minor amounts during the early postnatal period [31] and rises thereafter gradually until adulthood [28,31]. Analysis of CK activity during rat heart postnatal growth in whole tissue and mitochondrial homogenate has shown that MtCK is a major contributor to enhanced CK activity [40] and is thus responsible for the compartmentation of adenine nucleotides in mitochondria. Developmental activation of MM-CK has been investigated in several studies [31,41,42] and it has been found that MM-CK capacity to support myofibrillar ATPases is almost maximal already at postnatal day 3 [43].

During the maturation of cardiomyocytes, a number of changes occur parallel with the up regulation of MtCK: binding of MtCK to mitochondrial IMS, binding of MM-CK to myofibrils and compartmentalization of energy metabolites. Nevertheless, the available data on formation of ICEU and mechanisms responsible for the coupling of MtCK reaction with OXPHOS is still insufficient [28,43]. For example, regular mitochondrial arrangement is established within 3 postnatal weeks both in mouse and rat heart, while the value of $K^{app}{}_m$ADP continues to decrease up to 6 postnatal weeks [28,43].

The aim of this work was to study the formation of organized energy metabolism (ICEU) and maturation of mitochondrial respiration in cardiomyocytes during postnatal development and to elucidate the putative involvement of βII-tubulin in this process. The present study on rat cardiomyocytes combines functional and structural investigations to elucidate how maturation of the energetic system is paralleled with the structural changes during postnatal development and whether these structural changes are connected to the functional alteration.

2. Materials and methods

2.1. Laboratory animals and chemicals

Wistar rats at different ages (from day 1 postnatal to 6 months and in some experiments up to about 2 years) were used in the experiments. The animals were studied in accord with the "Guide for the Care and Use of Laboratory Animals" published by the US National Institute of Health (NIH publication no. 85-23, revised 1996). Animal procedures were approved by the Estonian National Committee for Ethics in Animal Experimentation (Estonian Ministry of Agriculture). All chemicals used in this study were from Roche, Fluka and Sigma-Aldrich.

2.2. Preparation of cardiac skinned fibers

Wistar rats were anesthetized; blood was protected against coagulation by injection of heparin. Rats were decapitated and the heart was quickly excised and skinned permeabilized cardiac fibers were prepared according to a method described earlier [44].

2.3. Isolation of cardiomyocytes

Calcium tolerant cardiomyocytes were isolated by perfusion with collagenase A (Roche) medium as described previously [14,16]. Flow-rate, perfusion pressure and size of cannula of Langendorf system was reduced and adapted for neonatal and young hearts. Isolated cardiomyocytes contained 70–90% of rod-like shaped cells.

2.4. Measurements of oxygen consumption

All experimental measurements of oxygen consumption were determined by a high-resolution respirometry Oxygraph-2K (OROBOROS Instruments, Innsbruck, Austria) in Mitomed solution [44] supplemented with 5 mM glutamate and 2 mM malate as respiratory substrates and 5 mg/mL essential fatty acid-free BSA. The respiration medium contains 3 mM inorganic phosphate (Pi), 3 mM Mg^{2+}, and saturating ADP concentrations are added to evaluate OXPHOS capacity (State 3). Measurements were carried out at 25 °C and respiration rates were expressed in $nmolO_2 \cdot min^{-1} \cdot mg \cdot protein^{-1}$. The permeabilization procedure for cardiomyocytes in all measurements of oxygen consumption was carried out directly in an oxygraph chamber with saponin (25 μg/mL) for 5 min before starting the measurements [44]. The intactness of mitochondrial membranes in isolated cardiomyocytes was validated by cytochrome *c* and carboxyatractyloside (CAT) tests for each experimental day [45]. Intactness of mitochondrial inner membrane (MIM) was checked with inhibiting adenine nucleotide carrier (ANT) by CAT. In cells with intact MIM the respiration rate decreased back to V_0 value. Only cells passing quality test were used in further experiments. In all presented data, the V_0 value was subtracted from the respiration rates. Activation of the mitochondrial respiration by the addition of exogenous cytochrome *c* did not exceed 10% of the maximal respiration rate (V_{max}). Respiratory control index (RCI) was measured in all observed ages.

Respiration kinetics for mitochondria was measured by adding ADP cumulatively and the maximum rates of respiration (V_{max}) and values for $K^{app}{}_m$ADP were calculated on the basis of the Michaelis–Menten equation.

Respiration rates for mitochondrial respiratory chain complexes were measured for the first time during postnatal development in cardiomyocytes by using a high-resolution respirometry Oxygraph-2K and method described earlier for isolated adult cardiomyocytes [44,46,47]. Mitochondrial respiration in cardiomyocytes was first activated by glutamate and malate as respiratory substrates via complex I (V_0 — basal respiration rate). Then the addition of ADP in saturating concentration (2 mM) activated mitochondrial respiration (V_{max}, maximal ADP-stimulated respiration rate or state 3 respiration rate). Thereafter, complex I was inhibited by its specific inhibitor rotenone (2.5 μM), an inhibitor for complex I of the respiratory chain. The addition of succinate (10 mM) reactivates oxygen consumption due to the succinate oxidation through complex II (succinate oxidase activity). Activation of succinate oxidase was followed by the addition of antimycin A (10 μM), an inhibitor of complex III. Finally, the addition of 1 mM *N*,*N*,*N*′,*N*′-tetramethyl-*p*-phenylenediamine (TMPD) and 5 mM ascorbate strongly activates the cytochrome *c* oxidase associated oxygen consumption rate. The addition of 1 mM sodium cyanide (NaCN) inhibits mitochondrial oxygen consumption. Respiration rate after addition of NaCN (non-mitochondrial consumption of O_2) was subtracted from TMPD respiration rate to correct for O_2 consumption associated with mitochondrial respiratory chain.

The functional maturation of the MtCK activity and CK energy transfer system in cardiomyocytes was measured experimentally at different postnatal ages by oxygraphic measurements in the presence of exogenous competitive enzyme system, consisting of 10 IU/ml of the pyruvate kinase (PK) and 5 mM of the phosphoenol pyruvate (PEP) [10]. In this experiment, at first, ATPases are activated by the addition of 2 mM ATP and thereby mitochondrial respiration is activated by ADP produced endogenously by ATPases. Thereafter, exogenously added PK-PEP system continuously traps all freely diffusing endogenously produced ADP. Afterwards, the MtCK and CK energy transfer system is activated by addition of 10 mM creatine [10,16]. Under these conditions kinetics of respiration follows the kinetics of MtCK reaction [48]. PEP–PK system removes extramitochondrial ADP produced by intracellular ATP-consuming reactions and continuously regenerates extramitochondrial ATP. Endogenous intramitochondrial ADP produced by MtCK forms microcompartments within the IMS and is re-imported into the matrix via ANT due to its functional coupling with MtCK [48].

2.5. Western blot analysis

Rat hearts were flash-frozen in liquid nitrogen and ground into fine powder with mortar and pestle. Soluble protein was extracted using Microtubule/Tubulin in vivo Assay Kit according to manufacturer's instructions (Cytoskeleton). Protein concentration was determined using the Pierce BCA Protein Kit (Thermo Scientific). Electrophoresis was performed on Mini Protean II from BioRad using tris–tricine buffer and 12% polyacrylamide gels. Proteins transfer was carried out for 1 h with 120 mA/membrane using PVDF membranes (Millipore) and semi-dry method [49]. Equal protein loading and transfer were verified by membrane staining with Ponceau solution (0.1% Ponceau S in 5% acetic acid) and additionally by total α-actin and total β-tubulin immunoblotting. However, since both aforementioned cytoskeletal proteins showed a tendency to decrease during the progression of heart development and were thus inadequate loading controls, Ponceau staining was taken as the most reliable indicator of an equal protein loading and transfer. All membranes were probed with Ponceau stain (see Fig. 1 in Supplemental material). The validity of Ponceau staining as a loading control and as an alternative to actin immunoblotting has been demonstrated elsewhere [50]. Total β-tubulin Western blotting was added aside from βII-tubulin and MtCK immunoblots as a loading control, although it also showed a tendency to decrease during development. Membranes were blocked for 1 h in 3% BSA/PBS for MtCK immunoblotting or in 1% skimmed milk/0.05% Tween-20 PBS solution, and probed with 1:250 anti-MtCK polyclonal antibody (Abcam, ab5596), 1:500 anti-β-tubulin polyclonal antibody (Abcam, ab6046) and 1:250 βII-tubulin monoclonal antibody (Abcam, ab28036). Immunoblots were detected by 1:45,000 anti-mouse or 1:1000 anti-rabbit secondary antibodies conjugated to peroxidase (IgG HRP; Abcam, ab97046 and ab6721-1, respectively) for 1 h at room temperature in the same buffers as the primary antibodies. Detection was conducted using a chemiluminescence kit (SuperSignal West Dura Extended Duration substrate).

2.6. Immunocytochemistry

Immunofluorescence staining of isolated rat cardiomyocytes or cardiac fibers was performed as previously described [23,51]. For βII-tubulin immunolabeling fibers were used instead of cardiomyocytes due to their more homogenous immunostaining of βII-tubulin, presumably due to the importance of cell-to-cell contact and integrity of plasma membrane in cytoskeletal organization [52]. For VDAC immunolabeling fixed cells/fibers were treated before permeabilization with Antigen Retrieval Buffer (10 mM Tris, 5% urea, pH 9.5) at 95 °C for 3 min. The following antibodies were used: mouse monoclonal antibody for βII-tubulin (Abcam, ab28036) at 1:250, rabbit monoclonal antibody for αIV-tubulin (Novus Biologicals, nb11057609) at 1:250, mouse monoclonal antibody for α-actinin (Abcam, ab82247) at 1:30, and rabbit polyclonal rabbit serum for VDAC (kindly provided Dr. Catherine Brenner, Université Paris-Sud, Paris, France) at 1:1000, DyLight 488 goat anti-rabbit IgG (Abcam, ab96899) at 1:250 and Dylight 549 goat anti-mouse IgG (Abcam, ab96880) at 1:250. Cells/fibers were mounted in ProLong® Gold Antifade Reagent with DAPI (Life Technologies), deposited on glass coverslips and observed by confocal microscope.

2.7. Image acquisition and processing

Fluorescence images were acquired by Zeiss LSM 510 confocal microscope (Carl Zeiss) equipped with a Plan-Apofluar 63×/1.3 glycerol objective and FluoView FV10i-W (Olympus) confocal microscope with 60×/1.2 water immersion objective. Laser excitation 489 nm was used for DyLight 488 with emission detected through a 505 to 530 nm band-pass filter; DyLight 549 was excited at 561 nm and detected through 575 to 615 nm band-pass filter. Processing of all confocal data sets was done with LSM Image Browser software and images were prepared for publication using Photoshop CS4 with no further modifications.

2.8. Statistical analysis

Results are expressed as the mean ± standard error of the mean (SEM). To determine statistical significance between age groups, analysis of ANOVA test was performed and p values less than 0.05 were considered significant. Correlation analysis was conducted for selected variables.

3. Results

Functional development of respiratory system and cytoarchitecture was studied in isolated rat cardiomyocytes at the ages from 1 day to adult (3 to 6 months).

3.1. Growth characteristics of rat cardiomyocytes during postnatal development

Change in body weight of rats at different ages is shown in Fig. 1A. Changes in cell shape during postnatal development of cardiomyocytes are depicted in transmission micrographs in Fig. 1B. At day 3, neonatal cells have round ends, spindle-like shape. Upon 10 days after birth, intracellular structure has become more organized and cell length increased. Alterations in the dimensions of isolated cardiomyocytes were measured from transmission confocal microscopy images (Fig. 1C). At postnatal day 3, cardiomyocytes were 75.4 ± 2.7 μm in length and 9.6 ± 0.3 μm in width; at postnatal day 10, 90.8 ± 4.5 μm in length and 18.8 ± 1.8 μm in width; and at 2 months, 127.6 ± 3.7 μm in length and 25.0 ± 3.2 μm in width. In comparison with these dimensions (Fig. 1C) and pictures of cardiomyocytes from 3, 10, and 57 day old rats (Fig. 1B) it is clear, that cells grow at first in length and then in width.

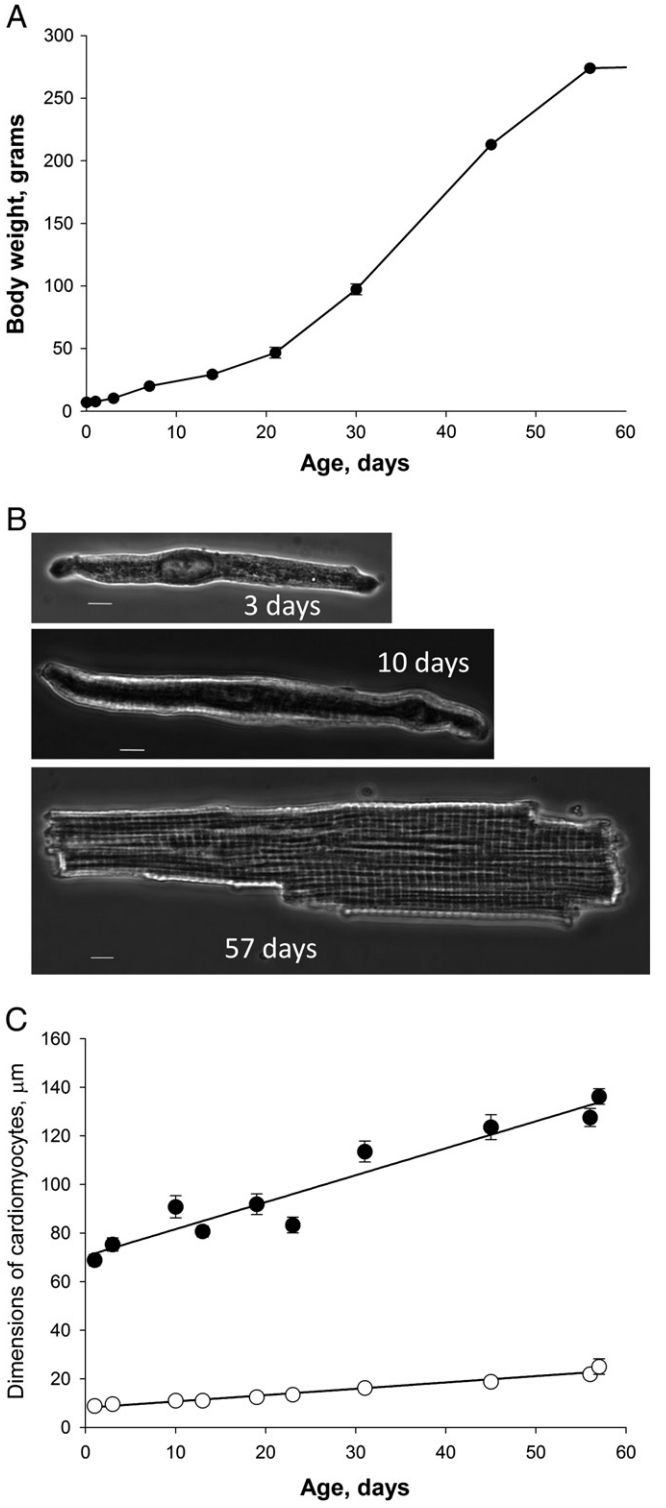

Fig. 1. Growth characteristics of rat heart. (A) Body weight of rat at different ages. (B) Transmission microscopy images of cardiomyocytes at different ages. Scale bar, 5 μM. (C) Size of rat cardiomyocytes: ● length ○ width. Results are means ± SEM. N ≥ 5.

3.2. Mitochondrial respiration in cardiomyocytes

Developmental changes in following respiration characteristics were studied: basal respiration rate (V_0, state 4 like respiration rate), maximal respiration rate (V_{max}ADP) in the presence of 2 mM ADP, respiratory control index (RCI) and $K^{app}{}_m$ADP (Fig. 2). V_{max}ADP and $K^{app}{}_m$ADP are rising progressively during postnatal development

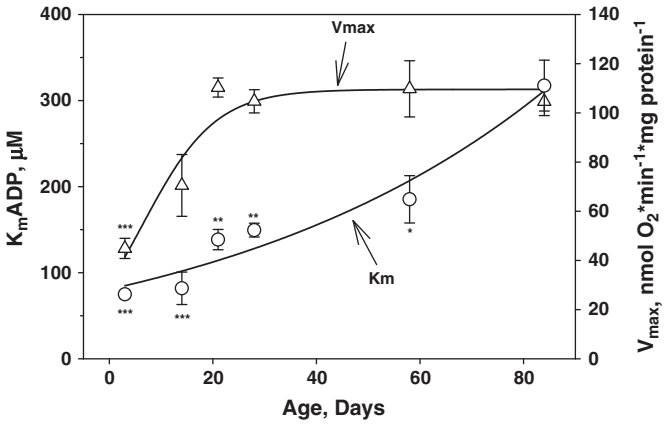

Fig. 2. Developmental changes in the values of maximal respiration rate and the apparent Km for exogenous ADP. Statistical significance: ***p < 0.001, **p < 0.01, *p < 0.05. Results are means ± SEM. N ≥ 5.

and adult-like values are reached at the age of 84 days. On the 3rd day after birth the maximal respiration rate in cardiomyocytes is 44.88 ± 4.12 nmol $O_2 \cdot min^{-1} \cdot mg\ protein^{-1}$ and $K^{app}{}_m$ADP of mitochondrial OXPHOS is 75.0 ± 4.5 μM. In contrast, in adult (at 84 days — about 3 months) these values were measured as 104.63 ± 5.72 nmol $O_2 \cdot min^{-1} \cdot mg\ protein^{-1}$ and 317.0 ± 29.5 μM, respectively.

3.3. Activities of the respiratory chain complexes

This study is the first to assess the developmental changes in the oxygen consumption for respiratory chain complexes in cardiomyocytes. Different substrates and inhibitors were used at one fixed concentration to analyze developmental changes in the activities of the respiratory chain complexes. Fig. 3A shows the original oxygraph recording from the investigation of the respiratory chain complexes in cardiomyocytes derived from 2-month-old rats. See Materials and methods for more details. Analysis of respiration rates for different respiratory chain complexes are shown in Fig. 3. At first, basal respiration rate (V_0, state 4 like respiration rate) was studied with respiratory substrates (glutamate and malate) (Fig. 3B). This value rose gradually and reached adult like level at the age of 1 month. The functioning of complex I (Fig. 3C) was assessed by stimulating the respiration with 2 mM ADP. The activity of complex I (ADP-simulated respiration) rose gradually with postnatal age as described earlier for V_{max} (Fig. 2). The values of the RCI, calculated from the respiration rates in Fig. 3B and C, did not significantly change during postnatal development (data not shown) due to concurrent rise in the basal (state 4 like) and maximal respiratory rate values (Fig. 3B,C).

To analyze changes in the activities of complex I and complex II, respiration was activated by the addition of ADP and succinate (Fig. 3C,D). Succinate was added after the inhibition of respiration by rotenone. Succinate oxidase activity (complex I dependent respiration) is higher than complex I during the early postnatal period (Fig. 3D) and reaches adult levels at second postnatal week. This shows the trend in direction of maturation of OXPHOS during postnatal development.

The addition of TMPD (an artificial substrate for complex IV of the respiratory chain) and ascorbate shows the maximal capacity of the respiratory chain (Fig. 3E). Respiration rates with TMPD reach the values close to those of the adult cardiomyocytes already after 2 weeks of postnatal development.

3.4. Mitochondrial creatine kinase function

Next, we examined the developmental expression of MtCK and its efficiency in mediating feed-back signaling with cytosolic ATPases. As developmental expression of myofibrillar CK has been assayed already in numerous previous reports [41–43], and rigor tension experiments have evidenced its maximal efficiency in supporting the activity of MgATPases being reached already at 3 days after birth [43], its role was not further analyzed in the current study. Western blot analysis (see Fig. 4A) demonstrates that MtCK is present at low levels already at postnatal day 3. However, more pronounced increase is visible around the second postnatal week, when MtCK expression achieves already ~60% of its adult level, and increases thereafter up to 21 days, which is in agreement with previously published data [38].

The activity of MtCK was studied by the addition of ATP and PK-PEP system to the oxygraphy measurements (see Materials and methods for more details). The original oxygraphy recording from MtCK activity is shown in Fig. 4B. At first 2 mM MgATP was added to activate the ATPases and to stimulate thereby mitochondrial respiration by endogenously produced ADP. If Cr (20 mM) is not added to activate MtCK, then addition of PK-PEP system evokes significant decline in the mitochondrial respiration rate due to the rapid rephosphorylation of extramitochondrial ADP (Fig. 4B). The PK-PEP system traps ADP and is able to reduce respiration rate up to 80%, when the CK system is not activated as already shown earlier for adult cardiomyocytes [53]. At postnatal day 3, stimulatory effect of Cr on mitochondrial respiration is absent and addition of PK/PEP evokes substantial decline in respiration rate (Fig. 4C). Thus, at early postnatal period creatine mediated feedback signaling is immature. On the other hand, clear activation of MtCK occurs at later stage (Fig. 4C), when endogenously channeled ADP becomes increasingly less accessible to the PK/PEP system and Cr becomes more capacitative in increasing the respiration rate in the presence of the PK/PEP system. Activation of respiration by Cr activation increased progressively from 14 to 84 postnatal days and become only then equal to adult levels (Fig. 4C).

3.5. Development of intracellular energetic units

To estimate the role of mitochondrial arrangement in maturation of mitochondrial respiration regulation, we immunolabeled mitochondria and Z-lines with antibodies against VDAC and α-actinin, respectively. The alterations in mitochondrial arrangement were assessed by confocal microscopy. Fig. 5A shows confocal micrographs of cardiomyocytes isolated at 8 and 21 days postnatal and adult rat heart. Significant remodeling of mitochondrial arrangement occurred during first postnatal weeks. At postnatal day 3, mitochondria are predominantly clustered around nuclei or irregularly dispersed around the cellular interior, while Z-lines are present primarily at subsarcolemmal areas. At postnatal day 21, mitochondria fill cellular interior more regularly and form parallel arrays within intermyofibrillar space. Thereafter, slight improvements in mitochondrial arrangement appear, mainly in terms of overall uniformity and in density. Thus, major changes in arrangement of mitochondria are completed within 3 postnatal weeks, which is in agreement with earlier electron microscopy observation with mouse heart [43].

To test if progressive change in the kinetics of mitochondrial respiration regulation by exogenous ADP can be explained by the alterations in location of mitochondria relative to βII-tubulin, we examined their arrangement in the cardiac fibers immunolabelled with antibodies against VDAC and βII-tubulin. Fibers were used instead on isolated cells due to their more homogenous βII-tubulin immunolabeling. Differences between respirometric characteristics of the cardiac fibers and isolated cardiomyocytes are marginal, as confirmed in this study and also shown before [28]. Fig. 5B shows confocal micrographs of cardiomyocytes isolated from 3, 14 and 21 day old and an adult rat hearts. Similar to α-actinin, βII-tubulin localized mainly in the cell periphery at early postnatal developmental stage and is clearly distant from the mitochondria, which are clustered predominantly at the perinuclear areas, as already evidenced above. At 14 postnatal day, βII-tubulin is expanded throughout the cellular interior and displays frequent disjunctions in place of mitochondrial array. Only at 21

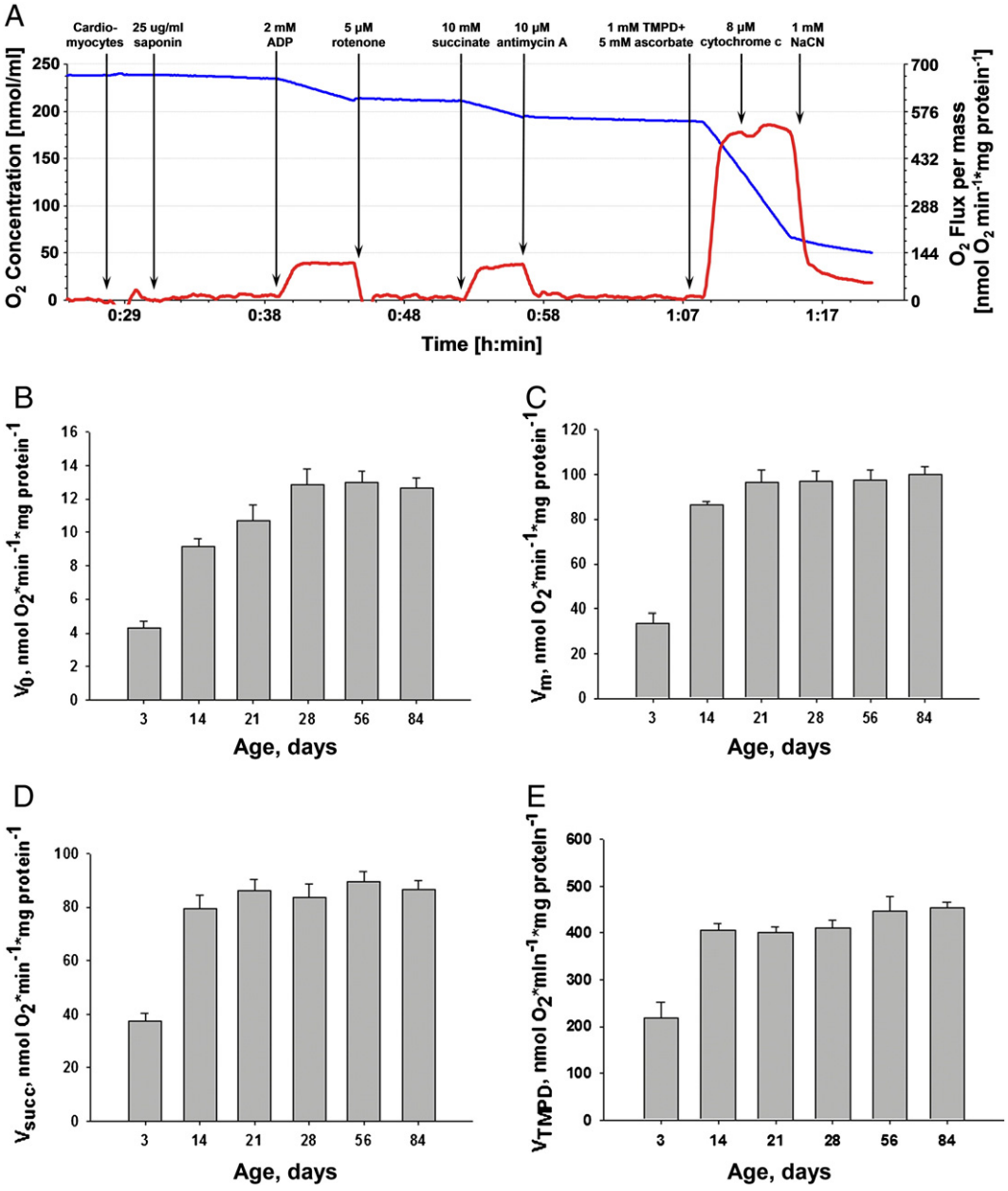

Fig. 3. Changes in respiratory chain activities during heart postnatal development. (A) Oxygraph recording of the activity of respiratory chain at the age of 2 months. Addition of 25 μg/mL saponin, 2 mM ADP, 5 mM rotenone, 10 mM succinate, 10 μM antimycin A (antimycin) and 1 mM N,N,N′,N′-tetramethyl-p-phenylenediamine (TMPD) with 5 mM ascorbate (Asc), 8 μM cytochrome *c* (cyt *c*) and 1 mM sodium cyanide (NaCN) to the oxygraph chamber. (B) V_0, basal respiration rate (state 4 like respiration rate) in the presence of substrates 5 mM glutamate and 2 mM malate. (C) V_{max}ADP, maximal respiration rate after the addition of 2 mM ADP (state 3 like respiration rate). (D) $V_{succinate}$, state 3 like respiration rate after the addition of 10 mM succinate. (E) V_{TMPD}, Respiration rate after the addition of 1 mM TMPD with 5 mM ascorbate. All results are means ± SEM. N ≥ 5.

postnatal day, alignment of mitochondria along βII-tubulin bundles starts to appear and βII-tubulin becomes more concentrated at intermyofibrillar space. Interestingly, significant accumulation of βII-tubulin to the cell tips was also visible during the first postnatal weeks and distribution of βII-tubulin appeared to follow the expansion of myofibrils.

Increase in free tubulin content is found to suppress metabolite influx to the mitochondria in a variety of cancerous and non-cancerous cell lines [22]. To test if developmental decline in the MOM permeability for ADP correlates with an increase in the levels of free βII-tubulin or total β-tubulin protein, we assessed their expression by Western blotting. Surprisingly, βII-tubulin protein level decreased almost 3-fold between 3 and 56 days and while total β-tubulin levels declined as well, it appeared to be less pronounced than for βII-tubulin (Fig. 5C). A similar observation was previously made on feline heart and reflects presumably their incorporation into stable microtubular network [54]. In addition, we observed an increase in the density of one higher Mw band (~60 kDa) on β-tubulin immunoblot that may correspond to one of its post-translationally modified forms. Nevertheless, these results show that changes in MOM permeability for ADP cannot be explained by the increase in βII- or total β-tubulin levels, which are both decreasing instead.

Additionally, localization of βII- and αIV-tubulin was studied in cardiomyocytes during postnatal development (Fig. 6A). From these micrographs, it is visible that localization of βII- and αIV-tubulin varies during development. The αIV-tubulin is localized close to the nucleus whereas βII-tubulin is localized in the periphery of cardiomyocytes during early postnatal period. Controversially, βII- and αIV-tubulins are distributed uniformly and in highly organized manner within cellular interior in the adult cardiomyocytes

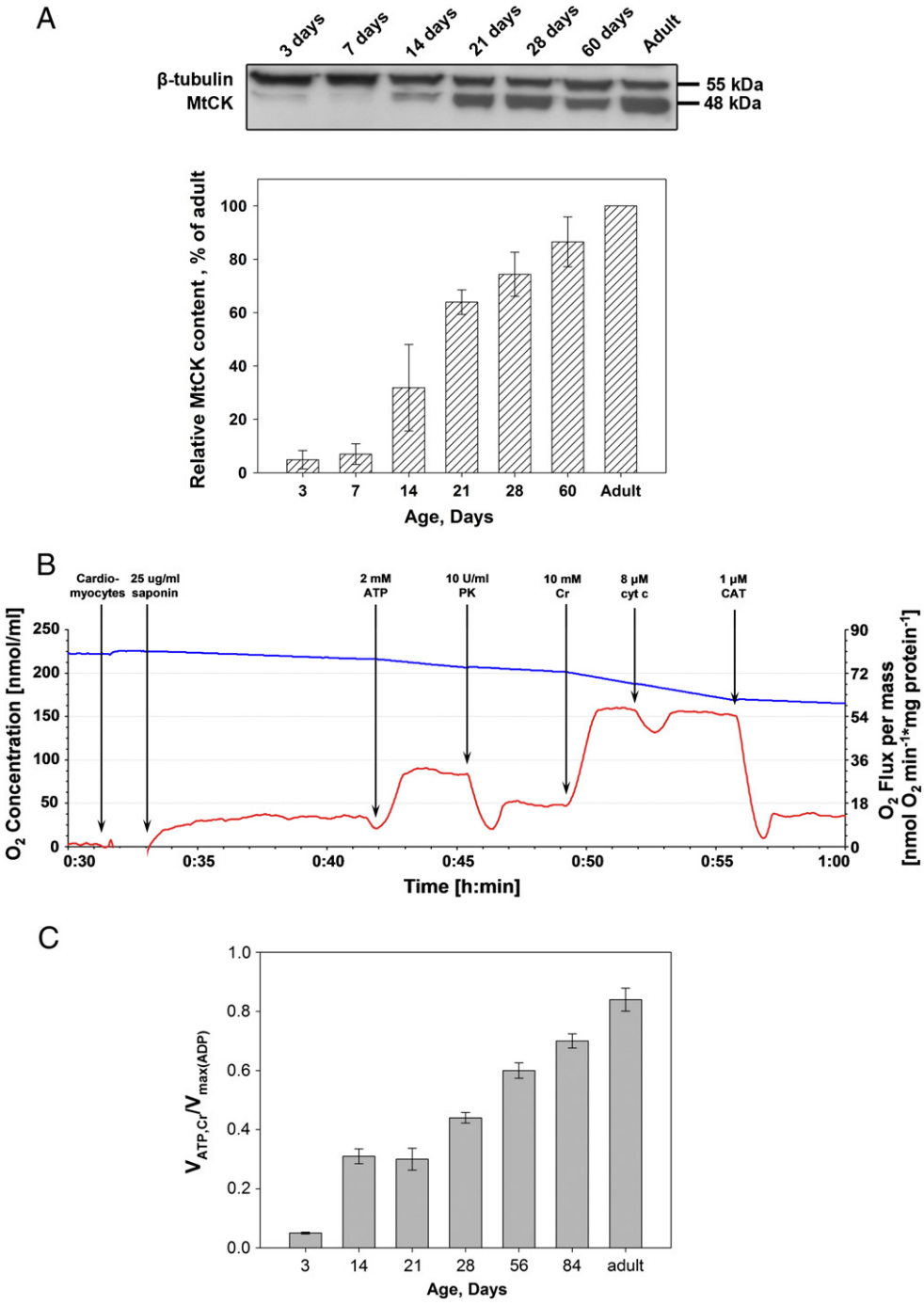

Fig. 4. Activation of the MtCK and phosphotransfer system during heart postnatal development. (A) Upper panel, Western blot analysis of MtCK and β-tubulin expression at different ages (25 μg protein per lane; n = 3 for each age). Lower panel, densitometric quantification of Western blot. Percentage of MtCK protein expression relative to adult. (B) The original recording from experiment with competitive PK-PEP system and addition of the creatine at postnatal day 33. (C) Increasing stimulatory effect of creatine on the respiration rate of cardiomyocytes in the presence of 2 mM ATP and competitive PEP-PK-system. V_{max}(ADP) — theoretical maximal respiration rate in the presence of exogenous ADP (see Fig. 2). ANOVA test showed that the differences between the relative stimulatory effect of creatine in age groups are statistically important ($p < 0.05$). Results are means ± SEM. $N \geq 5$.

(Fig. 6A). Pearson correlation coefficients for colocalization of βII- and αIV-tubulins were calculated. Fig. 6B is demonstrating the correlation between colocalization of tubulin isoforms and $K^{app}{}_m$ADP in mitochondrial respiration.

4. Discussion

The results of this study show that during cardiac postnatal development major alterations occur both in the intracellular architecture and

Fig. 5. Developmental organization of intracellular energetic units in cardiac cells at different ages. (A) Immunofluorescence micrographs of developmental distribution of mitochondria relative to Z-lines in cardiac fibers co-immunolabelled for α-actinin (DyLight 549, red) and VDAC (DyLight 488, green). (B) Immunofluorescence confocal micrographs of developmental distribution of mitochondrial and βII tubulin distribution in fibers co-immunolabelled for VDAC (DyLight 488, green) and βII tubulin (DyLight 549, red). Scale bar, 5 μm. (C) Upper panel, Western blot analysis of βII-tubulin and total β-tubulin (25 μg protein per lane; n = 3 for each age). Lower panel, densitometric quantification of Western blot. Percentage of βII-tubulin protein expression relative to adult. Results are means ± SEM.

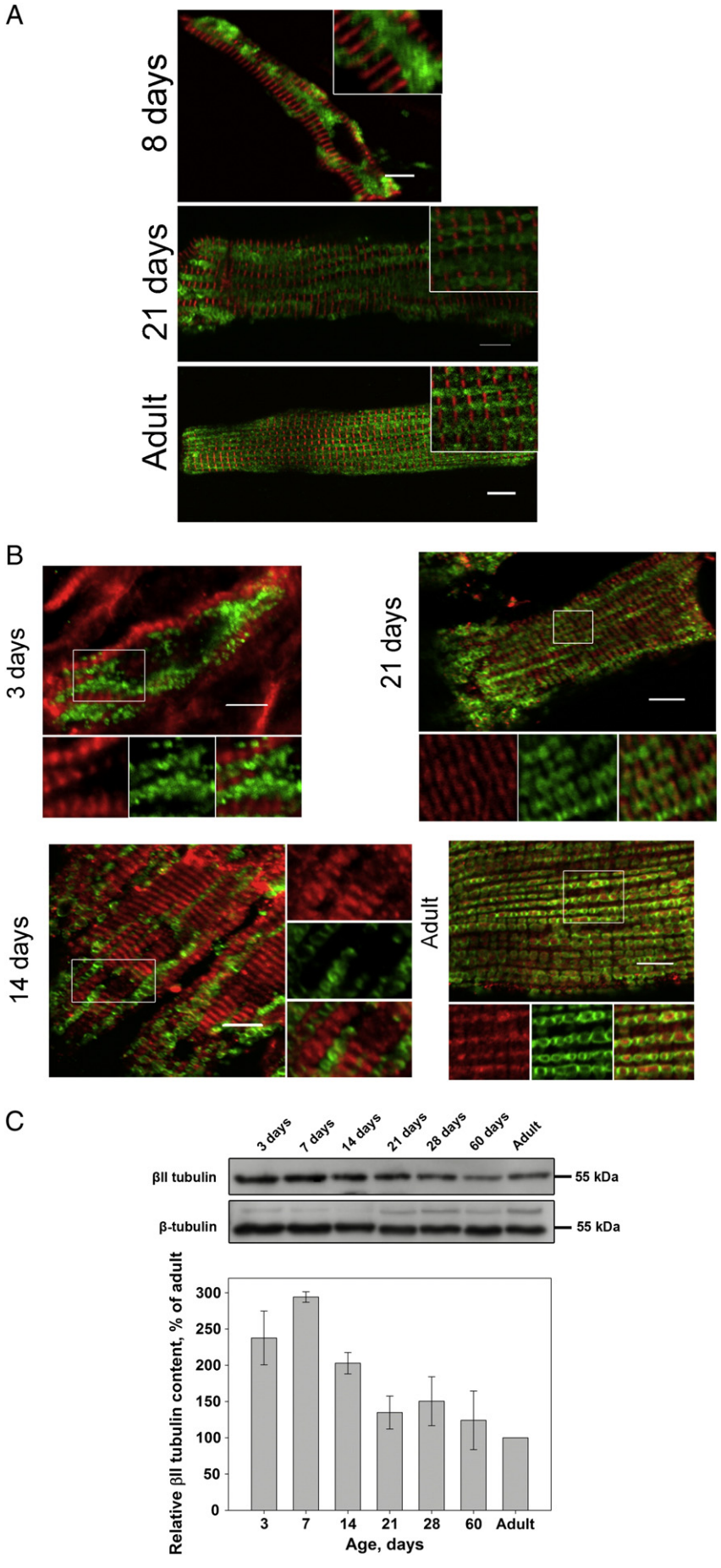
A
8 days
21 days
Adult
B
3 days
21 days
14 days
Adult
C
3 days
7 days
14 days
21 days
28 days
60 days
Adult
βII tubulin
55 kDa
β-tubulin
55 kDa
Relative βII tubulin content, % of adult
300
250
200
150
100
50
0
3
7
14
21
28
60
Adult
Age, days

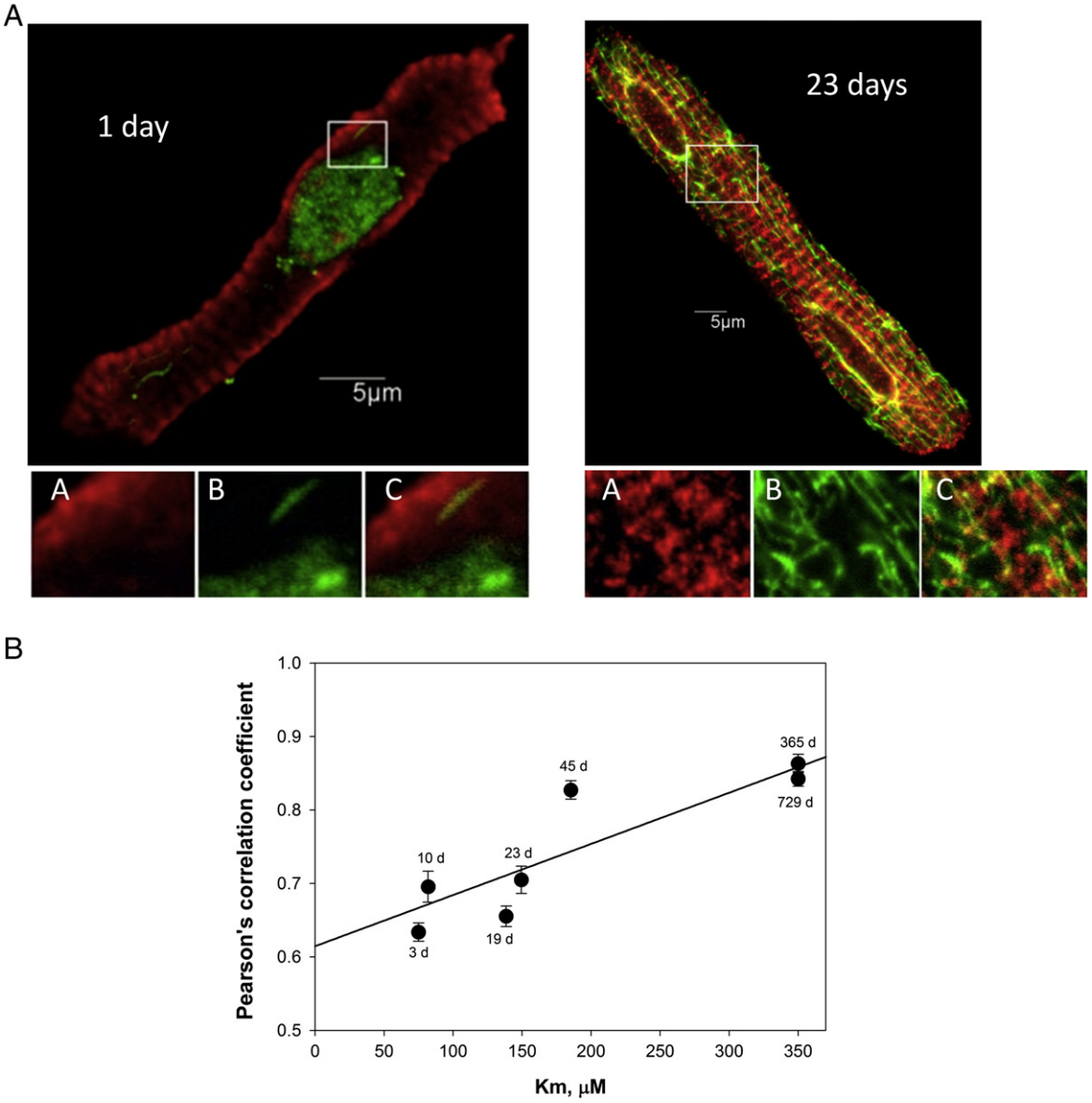

Fig. 6. Developmental alterations in colocalization of βII- and αIV-tubulin in cardiac cells at different ages. (A) Immunofluorescence confocal micrographs of βII- and αIV-tubulin distribution in cardiac cells co-immunolabelled for αIV-tubulin (DyLight 488, green) and βII-tubulin (DyLight 549, red). Scale bar, 5 μM. In all figures, one image of the z-stack from the approximate center of the cells is shown. (B) Correlation between Pearson's coefficients and $K^{app}{}_{m}$ADP. Pearson's correlation coefficients of colocalization of βII-tubulin and αIV-tubulin were calculated for at least eight image stacks (slide thickness 1 μm) containing 15–20 cells. Error bars: SEM.

in the functional level of energy metabolism. A gradual shift toward oxidative metabolism occurs in parallel with the increase in the cell size. Functional analysis of respiration regulation during postnatal development revealed further alterations in accessibility of exogenous ADP to the mitochondria and in PK/PEP suggesting that spatial positioning of the mitochondria is not the only determinant in the functional maturation of feedback regulation and that interactions with cytoskeletal proteins are probably involved.

Analysis of mitochondrial respiration, activated by ADP, showed that the maximal respiration rate increases continuously in parallel with the basal respiration rate (Figs. 2 and 3C). This is presumably related to growing volume and density of mitochondria as well as to increasing activity of the respiratory chain segments, as demonstrated in many earlier studies [53,55,56]. One of the key regulators of mitochondrial biogenesis in mitochondria rich tissues, such as heart and skeletal muscles, is a transcription coactivator PGC1α (peroxisome proliferator-activated receptor γ coactivator-1α), that is upregulated during heart postnatal period in response to changes in various extra and intracellular signals (e.g. FFA, Ca^{2+}, thyroid hormone, insulin, ATP demand, etc.) and stimulates mitochondrial DNA replication and transcription [57,58]. Its overexpression in myoblasts is shown to increase mRNAs for several genes of OXPHOS pathway [59] and cause dramatic increase in mitochondrial number and size in neonatal heart [60], explaining thus the observed increase in overall respiratory capacity seen in this study. Since RCI values (data not shown) were not significantly changing during development, it can be concluded that changes in respiratory rates are reflecting quantitative rather than qualitative fine-tuning of OXPHOS.

Interestingly, analysis of activities of the respiratory chain complexes revealed additional stimulatory effect of succinate (a substrate for complex II) on the respiration rate during the first postnatal week (Fig. 3C,D). Importantly, activity of complex I is markedly higher than that of complex II in adult cardiomyocytes [16,44,61], suggesting that during early postnatal period NAD-linked respiration is deficient. A similar observation has been previously made in HL-1 cells [46,47], cancer cells [62–65] and in the case of cardiac disease [61,66]. One of the likely reasons for this is the prevalence of glycolysis during early postnatal

period that produces reducing equivalents for complex II. After birth, cardiac cells encounter significant changes in their extracellular environment and workload conditions, to which they adapt by shifting gradually toward oxidative metabolism. These adaptations are elicited by decreasing levels of blood lactate and by rise in oxygen and FFA availability, accompanied by changes in various hormonal levels (e.g. thyroid hormone, insulin and glucagon). Immediate rise in blood glucagon levels after birth is shown to promote the increase in myocardial cAMP levels and activates pyruvate kinase A (PKA) [33]. The latter in turn, targets many mitochondrial proteins, including a subunit of complex I encoded by nuclear gene NDUFS4 [67]. In fibroblast and myoblast cultures cAMP dependent phosphorylation of this protein is associated with stimulation of complex I and overall respiration activity with NAD-linked substrates [67]. In addition, genes encoding for complex I subunits are known to respond to thyroid hormone signaling cascade, which is another cardiac mitochondrial biogenesis stimulating pathway activated during physiological heart growth [68]. Our results agree well with these observations and demonstrate that the role of OXPHOS in energy metabolism is progressively increasing during cardiac postnatal development accompanied by the rising importance of complex I linked respiration.

Analysis of Cr-stimulated respiration evidenced a significant enhancement in the efficiency of coupling between MtCK and OXPHOS reactions during postnatal heart development. After 14 postnatal days, Cr starts to elicit marked effect on mitochondrial respiration and becomes increasingly more potent in rescuing from PK/PEP induced inhibition of mitochondrial respiration (Fig. 4C). Continuous increase in Cr-stimulated respiration rate is observed up to 3 months postnatal, which might be thus regarded as the time-point when cardiomyocytes reach their full capacity in terms of energy metabolism. Cr exerts its effect on respiration by activating MtCK in IMS, that results in ATP/ADP cycling within mitochondria and prevents thereby the accessibility of endogenous ADP to extramitochondrial PK-PEP system. The observed increase in Cr-sensitive respiration rate during postnatal development shows that mitochondrial respiration inclines progressively toward Cr-based control that is realized through functionally coupled MtCK and OXPHOS reactions. The existence of such coupling in adult cardiac cells has been experimentally proven and described [48]. Piquereau et al. also claimed, based on electron microscopy and functional analysis, that organization of mitochondria in mouse cardiac cells is almost completed within 21 days postnatal while maturation of energy transfer from mitochondria to cytosolic ATPases continues to improve until the age of 2 months [43].

Previous studies have shown that the efficiency of metabolic feedback signaling between mitochondria and cytosolic ATP-ases over CK transfer system is significantly influenced by the arrangement of mitochondria [13]. Experiments with trypsin treated adult cardiomyocytes demonstrated that mitochondrial and cytoskeleton disorganization results in manifold increase in the respiratory affinity for ADP and cause pronounced decline in the efficiency of coupling between MtCK reaction and OXPHOS, as shown by PK-PEP test [69]. Our results here agree with these findings by demonstrating that the fidelity of metabolic feedback between mitochondria and cytosolic ATP-ases is improving in liaison with mitochondria localization relative to myofibrils and also to βII-tubulin. During early postnatal period, mitochondria are randomly clustered within the cytoplasm, distant from βII-tubulin, and most of the endogenously channeled ADP is accessible then to the PK/PEP system (Fig. 4C). Obviously, part of this accessibility is related to MtCK expression levels, which are relatively low at that time. Still, the notion that PK/PEP induced respiration inhibition is rescued by Cr much later than adult-like MtCK expression is achieved. This suggests clearly that additional cellular factors, such as mitochondrial localization and establishment of contacts between mitochondrial and cytoskeletal structures, are important for the maturation of this system (Fig. 4C).

Interestingly, the formation of diffusion restrictions for ADP showed rather slow maturation time, with $K^{app}{}_m$ADP values increasing gradually up to the age of 2 months (Fig. 2). However, some diffusion restrictions for ADP were clearly present already after birth, because the value of the $K^{app}{}_m$ADP at postnatal day 3 was already higher than in isolated adult cardiac mitochondria (i.e. 15–20 μM) [70]. Significant change in this value was observed, at second postnatal week when increase in MtCK expression level (Fig. 4A) and activity were observed (Fig. 4C). As MtCK localizes within the IMS, it is plausible that its accumulation into mitochondria may partly contribute to the changes in permeability of MOM for ADP. Still the main factor known to influence the diffusion restrictions for ADP, is mitochondrial–cytoskeletal interactions and binding of tubulin to VDAC [18,19].

Confocal microscopy analysis showed that during the first postnatal weeks, βII-tubulin distribution follows the myofibrillar expansion and is relatively independent from mitochondrial arrangement. However, after 3 postnatal weeks mitochondria start to align along the bundles βII-tubulin, accompanied by pronounced shift in $K^{app}{}_m$ADP of mitochondrial respiration and in improvement of Cr-mediated phosphotransfer. Concurrently, gradual decline also in free βII-tubulin levels is seen, as shown by Western blot analysis (Fig. 5A), pointing that availability of free βII-tubulin or total β-tubulin itself is not the determinant in regulation of VDAC permeability during heart development. According to the observation made by Narishige et al., decline in soluble βII-tubulin and total β-tubulin levels during heart development manifests tubulin stabilization and incorporation into stable microtubular lattice [54]. As microtubules represent the main tracks for subcellular mitochondrial distribution in upper eukaryotes, reconfiguration and stabilization of βII-tubulin may instead serve to promote the compartment-specific localization and docking of mitochondria in the vicinity of main energy consumption sites, contributing thereby to the establishment of ICEU.

Whether the trafficking of mitochondria at the level A-band within intermyofibrillar space is a necessary prerequisite for regulation of mitochondrial ADP sensitivity by the local pool of non-assembled βII-tubulin, was not revealed in this study. Obviously decline in βII-tubulin level cannot be accounted for increased diffusion restrictions for ADP of mitochondria and implicates that the regulation of VDAC closure encompasses either additional mechanisms or other binding partners. One of the plausible mechanisms may be that tubulin binding is related to certain VDAC isoforms, more abundantly expressed in later developmental stage. Evidence that different VDAC isoforms display distinct permeability characteristics have been received in studies with yeast and in VDAC deficient mice [23,71,72]. Additionally, modulation of VDAC phosphorylation could determine the extent of tubulin binding and explain the progressive decline in mitochondrial respiration affinity for ADP. For example, phosphorylation of VDAC by glycogen synthase kinase 3 beta (GSK3beta) or cAMP protein kinase, is shown to promote tubulin binding to VDAC and induce reduction in mitochondrial inner membrane potential [18,73]. This needs further study in the future.

Colocalization of βII- and αIV-tubulin isoforms (Fig. 6A) gradually rises during development and distribution of these isoforms is similar to the arrangement of mitochondria at 23 postnatal day. Existing correlation between $K^{app}{}_m$ADP of mitochondrial respiration and Pearson's coefficients for colocalization of tubulin isoforms might show the involvement of these proteins in the arrangement of mitochondria into the ICEU or involvement in the regulation of the permeability of MOM via binding to the VDAC channel. But this hypothesis about the role of βII- and αIV-tubulin in regulation of mitochondrial respiration needs further investigation in rat cardiomyocytes. Moreover, the role of α-tubulins in regulation of energy metabolism is still totally unknown. According to some recent theories, it could be C-terminal tail of α-tubulin that interact with the VDAC lumen decreasing its permeability for anions, while that of β-tubulin binds to VDAC binding site situated on the cytosolic

face [18,74,75]. Further studies are needed to determine the interactions between mitochondria and βII-tubulin/αIV-tubulin and to elucidate which other cytoskeletal proteins are involved in regulation of mitochondrial respiration.

Altogether these results show that diffusion restrictions for adenine nucleotides and coupling of MtCK reaction with OXPHOS is dependent on the positioning of mitochondria in the vicinity of myofibrillar ATPases, establishment of interaction between mitochondria and cytoskeletal proteins, and upregulation of MtCK [11,76]. Future studies need to address whether developmental decrease in MOM permeability in cardiomyocytes for ADP is related to the direct binding of tubulin to VDAC as a result of changes in VDAC phosphorylation level or isoform distribution.

5. Conclusions

Results of this study show that energy metabolism is mature at the level of OXPHOS much earlier than maturation of MtCK mediated feedback regulation and intracellular architecture occurs. We found that mitochondrial respiration affinity for ADP gradually decreases ($K^{app}{}_m$ADP rises from 75 to 300 μM) during development of cardiomyocytes. At the same time MtCK becomes progressively more capacitative in mediating the feedback signal between cytosolic ATPases and mitochondria. These functional alterations are accompanied by major changes in the arrangement of mitochondria relative to myofibrils and to the localization of cytoskeletal proteins and reconfiguration of βII- and αIV-tubulin subcellular arrangement. This shows the possible importance of cytoskeletal interactions with mitochondria in maturation of cardiac energy metabolism. These results highlight that functional maturity on the level of MtCK and mitochondrial respiration regulation is achieved after the maturation of intracellular architecture. This supports a model where energy metabolism is directly linked to the highly organized intracellular architecture in cardiomyocytes. In conclusion, rat heart is structurally and metabolically mature at the age of 3 month, when ICEU is fully formed and MtCK is active and forming microcompartmentation for production of PCr.

Supplementary data to this article can be found online at http://dx.doi.org/10.1016/j.bbabio.2014.03.015.

Acknowledgments

This work was supported by the Estonian Science Foundation grant no. 7823, the Estonian Ministry of Education and Research grant no. SF0180114Bs08 and the Estonian Research Council Institutional Research grant no. 23-1. We wish to acknowledge Maire Peitel for excellent technical assistance and Dr. Catherine Brenner (University of Paris-Sud, Paris, France) for kindly sending us antibodies for VDAC. We are very grateful to Madis Metsis for reading the manuscript and Andre Koit for review of English in the manuscript.

References

[1] A.M. Gordon, M. Regnier, E. Homsher, Skeletal and cardiac muscle contractile activation: tropomyosin "rocks and rolls", News Physiol. Sci. 16 (2001) 49–55.
[2] M. Vendelin, N. Beraud, K. Guerrero, T. Andrienko, A.V. Kuznetsov, J. Olivares, L. Kay, V.A. Saks, Mitochondrial regular arrangement in muscle cells: a "crystal-like" pattern, Am. J. Physiol. Cell Physiol. 288 (2005) C757–C767.
[3] T. Anmann, M. Eimre, A.V. Kuznetsov, T. Andrienko, T. Kaambre, P. Sikk, E. Seppet, T. Tiivel, M. Vendelin, V.A. Saks, Calcium-induced contraction of sarcomeres changes the regulation of mitochondrial respiration in permeabilized cardiac cells, FEBS J. 272 (2005) 3145–3161.
[4] V.A. Saks, T. Kaambre, P. Sikk, M. Eimre, E. Orlova, K. Paju, A. Piirsoo, F. Appaix, L. Kay, V. Regitz-Zagrosek, E. Fleck, E. Seppet, Intracellular energetic units in red muscle cells, Biochem. J. 356 (2001) 643–657.
[5] E.K. Seppet, T. Kaambre, P. Sikk, T. Tiivel, H. Vija, M. Tonkonogi, K. Sahlin, L. Kay, F. Appaix, U. Braun, M. Eimre, V.A. Saks, Functional complexes of mitochondria with Ca,MgATPases of myofibrils and sarcoplasmic reticulum in muscle cells, Biochim. Biophys. Acta 1504 (2001) 379–395.
[6] A. Kaasik, V. Veksler, E. Boehm, M. Novotova, A. Minajeva, R. Ventura-Clapier, Energetic crosstalk between organelles: architectural integration of energy production and utilization, Circ. Res. 89 (2001) 153–159.
[7] V. Saks, A.V. Kuznetsov, M. Gonzalez-Granillo, K. Tepp, N. Timohhina, M. Karu-Varikmaa, T. Kaambre, P. Dos Santos, F. Boucher, R. Guzun, Intracellular energetic units regulate metabolism in cardiac cells, J. Mol. Cell. Cardiol. 52 (2012) 419–436.
[8] V. Saks, R. Guzun, N. Timohhina, K. Tepp, M. Varikmaa, C. Monge, N. Beraud, T. Kaambre, A. Kuznetsov, L. Kadaja, M. Eimre, E. Seppet, Structure–function relationships in feedback regulation of energy fluxes *in vivo* in health and disease: mitochondrial interactosome, Biochim. Biophys. Acta 1797 (2010) 678–697.
[9] V. Saks, T. Kaambre, R. Guzun, T. Anmann, P. Sikk, U. Schlattner, T. Wallimann, M. Aliev, M. Vendelin, The creatine kinase phosphotransfer network: thermodynamic and kinetic considerations, the impact of the mitochondrial outer membrane and modelling approaches, Subcell. Biochem. 46 (2007) 27–65.
[10] N. Timohhina, R. Guzun, K. Tepp, C. Monge, M. Varikmaa, H. Vija, P. Sikk, T. Kaambre, D. Sackett, V. Saks, Direct measurement of energy fluxes from mitochondria into cytoplasm in permeabilized cardiac cells in situ: some evidence for mitochondrial interactosome, J. Bioenerg. Biomembr. 41 (2009) 259–275.
[11] F. Appaix, A.V. Kuznetsov, Y. Usson, L. Kay, T. Andrienko, J. Olivares, T. Kaambre, P. Sikk, R. Margreiter, V. Saks, Possible role of cytoskeleton in intracellular arrangement and regulation of mitochondria, Exp. Physiol. 88 (2003) 175–190.
[12] T. Anmann, R. Guzun, N. Beraud, S. Pelloux, A.V. Kuznetsov, L. Kogerman, T. Kaambre, P. Sikk, K. Paju, N. Peet, E. Seppet, C. Ojeda, Y. Tourneur, V. Saks, Different kinetics of the regulation of respiration in permeabilized cardiomyocytes and in HL-1 cardiac cells. Importance of cell structure/organization for respiration regulation, Biochim. Biophys. Acta 1757 (2006) 1597–1606.
[13] J.R. Wilding, F. Joubert, C. de Araujo, D. Fortin, M. Novotova, V. Veksler, R. Ventura-Clapier, Altered energy transfer from mitochondria to sarcoplasmic reticulum after cytoarchitectural perturbations in mice hearts, J. Physiol. 575 (2006) 191–200.
[14] V.A. Saks, Y.O. Belikova, A.V. Kuznetsov, *In vivo* regulation of mitochondrial respiration in cardiomyocytes: specific restrictions for intracellular diffusion of ADP, Biochim. Biophys. Acta 1074 (1991) 302–311.
[15] R. Guzun, N. Timohhina, K. Tepp, C. Monge, T. Kaambre, P. Sikk, A.V. Kuznetsov, C. Pison, V. Saks, Regulation of respiration controlled by mitochondrial creatine kinase in permeabilized cardiac cells in situ. Importance of system level properties, Biochim. Biophys. Acta 1787 (2009) 1089–1105.
[16] K. Tepp, I. Shevchuk, V. Chekulayev, N. Timohhina, A.V. Kuznetsov, R. Guzun, V. Saks, T. Kaambre, High efficiency of energy flux controls within mitochondrial interactosome in cardiac intracellular energetic units, Biochim. Biophys. Acta 1807 (2011) 1549–1561.
[17] L. Kay, Z. Li, M. Mericskay, J. Olivares, L. Tranqui, E. Fontaine, T. Tiivel, P. Sikk, T. Kaambre, J.L. Samuel, L. Rappaport, Y. Usson, X. Leverve, D. Paulin, V.A. Saks, Study of regulation of mitochondrial respiration *in vivo*. An analysis of influence of ADP diffusion and possible role of cytoskeleton, Biochim. Biophys. Acta 1322 (1997) 41–59.
[18] K.L. Sheldon, E.N. Maldonado, J.J. Lemasters, T.K. Rostovtseva, S.M. Bezrukov, Phosphorylation of voltage-dependent anion channel by serine/threonine kinases governs its interaction with tubulin, PLoS One 6 (2011) e25539.
[19] T.K. Rostovtseva, K.L. Sheldon, E. Hassanzadeh, C. Monge, V. Saks, S.M. Bezrukov, D.L. Sackett, Tubulin binding blocks mitochondrial voltage-dependent anion channel and regulates respiration, Proc. Natl. Acad. Sci. U. S. A. 105 (2008) 18746–18751.
[20] M. Carre, N. Andre, G. Carles, H. Borghi, L. Brichese, C. Briand, D. Braguer, Tubulin is an inherent component of mitochondrial membranes that interacts with the voltage-dependent anion channel, J. Biol. Chem. 277 (2002) 33664–33669.
[21] C. Monge, N. Beraud, A.V. Kuznetsov, T. Rostovtseva, D. Sackett, U. Schlattner, M. Vendelin, V.A. Saks, Regulation of respiration in brain mitochondria and synaptosomes: restrictions of ADP diffusion in situ, roles of tubulin, and mitochondrial creatine kinase, Mol. Cell. Biochem. 318 (2008) 147–165.
[22] E.N. Maldonado, J. Patnaik, M.R. Mullins, J.J. Lemasters, Free tubulin modulates mitochondrial membrane potential in cancer cells, Cancer Res. 70 (2010) 10192–10201.
[23] M. Varikmaa, R. Bagur, T. Kaambre, A. Grichine, N. Timohhina, K. Tepp, I. Shevchuk, V. Chekulayev, M. Metsis, F. Boucher, V. Saks, A.V. Kuznetsov, R. Guzun, Role of mitochondria–cytoskeleton interactions in respiration regulation and mitochondrial organization in striated muscles, Biochim. Biophys. Acta 1837 (2014) 232–245.
[24] A.V. Kuznetsov, S. Javadov, R. Guzun, M. Grimm, V. Saks, Cytoskeleton and regulation of mitochondrial function: the role of beta-tubulin II, Front. Physiol. 4 (2013) 82.
[25] A. Banerjee, M.C. Roach, K.A. Wall, M.A. Lopata, D.W. Cleveland, R.F. Luduena, A monoclonal antibody against the type II isotype of beta-tubulin. Preparation of isotypically altered tubulin, J. Biol. Chem. 263 (1988) 3029–3034.
[26] X.H. Jaglin, J. Chelly, Tubulin-related cortical dysgeneses: microtubule dysfunction underlying neuronal migration defects, Trends Genet. 25 (2009) 555–566.
[27] G.A. Porter Jr., J. Hom, D. Hoffman, R. Quintanilla, K. de Mesy Bentley, S.S. Sheu, Bioenergetics, mitochondria, and cardiac myocyte differentiation, Prog. Pediatr. Cardiol. 31 (2011) 75–81.
[28] T. Tiivel, L. Kadaya, A. Kuznetsov, T. Kaambre, N. Peet, P. Sikk, U. Braun, R. Ventura-Clapier, V. Saks, E.K. Seppet, Developmental changes in regulation of mitochondrial respiration by ADP and creatine in rat heart *in vivo*, Mol. Cell. Biochem. 208 (2000) 119–128.
[29] A. Bass, M. Stejskalova, A. Stieglerova, B. Ostadal, M. Samanek, Ontogenetic development of energy-supplying enzymes in rat and guinea-pig heart, Physiol. Res. 50 (2001) 237–245.
[30] G.D. Lopaschuk, J.S. Jaswal, Energy metabolic phenotype of the cardiomyocyte during development, differentiation, and postnatal maturation, J. Cardiovasc. Pharmacol. 56 (2010) 130–140.

[31] A. Fischer, M. Ten Hove, L. Sebag-Montefiore, H. Wagner, K. Clarke, H. Watkins, C.A. Lygate, S. Neubauer, Changes in creatine transporter function during cardiac maturation in the rat, BMC Dev. Biol. 10 (2010) 70.
[32] R.J. Ascuitto, N.T. Ross-Ascuitto, Substrate metabolism in the developing heart, Semin. Perinatol. 20 (1996) 542–563.
[33] A.O. Makinde, P.F. Kantor, G.D. Lopaschuk, Maturation of fatty acid and carbohydrate metabolism in the newborn heart, Mol. Cell. Biochem. 188 (1998) 49–56.
[34] A. Boneh, Regulation of mitochondrial oxidative phosphorylation by second messenger-mediated signal transduction mechanisms, Cell. Mol. Life Sci. 63 (2006) 1236–1248.
[35] M.R. Duchen, A. Leyssens, M. Crompton, Transient mitochondrial depolarizations reflect focal sarcoplasmic reticular calcium release in single rat cardiomyocytes, J. Cell Biol. 142 (1998) 975–988.
[36] R. Garesse, C.G. Vallejo, Animal mitochondrial biogenesis and function: a regulatory cross-talk between two genomes, Gene 263 (2001) 1–16.
[37] A. Ikenishi, H. Okayama, N. Iwamoto, S. Yoshitome, S. Tane, K. Nakamura, T. Obayashi, T. Hayashi, T. Takeuchi, Cell cycle regulation in mouse heart during embryonic and postnatal stages, Dev. Growth Differ. 54 (2012) 731–738.
[38] N. Hall, M. DeLuca, Developmental changes in creatine phosphokinase isoenzymes in neonatal mouse hearts, Biochem. Biophys. Res. Commun. 66 (1975) 988–994.
[39] J.S. Ingwall, W.R. Roeske, K. Wildenthal, The fetal mouse heart in organ culture: maintenance of the differentiated state, Methods Cell Biol. 21A (1980) 167–186.
[40] R.T. Dowell, Mitochondrial component of the phosphorylcreatine shuttle is enhanced during rat heart perinatal development, Biochem. Biophys. Res. Commun. 141 (1986) 319–325.
[41] R.V. Trask, J.J. Billadello, Tissue-specific distribution and developmental regulation of M and B creatine kinase mRNAs, Biochim. Biophys. Acta 1049 (1990) 182–188.
[42] R.T. Dowell, M.C. Fu, Heterogeneous cellular expression of creatine kinase isoenzyme during normal rat heart development, Mol. Cell. Biochem. 178 (1998) 87–94.
[43] J. Piquereau, M. Novotova, D. Fortin, A. Garnier, R. Ventura-Clapier, V. Veksler, F. Joubert, Postnatal development of mouse heart: formation of energetic microdomains, J. Physiol. 588 (2010) 2443–2454.
[44] A.V. Kuznetsov, V. Veksler, F.N. Gellerich, V. Saks, R. Margreiter, W.S. Kunz, Analysis of mitochondrial function in situ in permeabilized muscle fibers, tissues and cells, Nat. Protoc. 3 (2008) 965–976.
[45] V.A. Saks, V.I. Veksler, A.V. Kuznetsov, L. Kay, P. Sikk, T. Tiivel, L. Tranqui, J. Olivares, K. Winkler, F. Wiedemann, W.S. Kunz, Permeabilized cell and skinned fiber techniques in studies of mitochondrial function *in vivo*, Mol. Cell. Biochem. 184 (1998) 81–100.
[46] M. Eimre, K. Paju, S. Pelloux, N. Beraud, M. Roosimaa, L. Kadaja, M. Gruno, N. Peet, E. Orlova, R. Remmelkoor, A. Piirsoo, V. Saks, E. Seppet, Distinct organization of energy metabolism in HL-1 cardiac cell line and cardiomyocytes, Biochim. Biophys. Acta 1777 (2008) 514–524.
[47] C. Monge, N. Beraud, K. Tepp, S. Pelloux, S. Chahboun, T. Kaambre, L. Kadaja, M. Roosimaa, A. Piirsoo, Y. Tourneur, A.V. Kuznetsov, V. Saks, E. Seppet, Comparative analysis of the bioenergetics of adult cardiomyocytes and nonbeating HL-1 cells: respiratory chain activities, glycolytic enzyme profiles, and metabolic fluxes, Can. J. Physiol. Pharmacol. 87 (2009) 318–326.
[48] R. Guzun, N. Timohhina, K. Tepp, M. Gonzalez-Granillo, I. Shevchuk, V. Chekulayev, A.V. Kuznetsov, T. Kaambre, V.A. Saks, Systems bioenergetics of creatine kinase networks: physiological roles of creatine and phosphocreatine in regulation of cardiac cell function, Amino Acids 40 (2011) 1333–1348.
[49] J. Sambrook, D.W. Russell, Molecular Cloning: A Laboratory Manual, 3rd ed. Cold Spring Harbor Laboratory Press, Cold Spring Harbor, N.Y., 2001
[50] I. Romero-Calvo, B. Ocon, P. Martinez-Moya, M.D. Suarez, A. Zarzuelo, O. Martinez-Augustin, F.S. de Medina, Reversible Ponceau staining as a loading control alternative to actin in Western blots, Anal. Biochem. 401 (2010) 318–320.
[51] R. Guzun, M. Gonzalez-Granillo, M. Karu-Varikmaa, A. Grichine, Y. Usson, T. Kaambre, K. Guerrero-Roesch, A. Kuznetsov, U. Schlattner, V. Saks, Regulation of respiration in muscle cells *in vivo* by VDAC through interaction with the cytoskeleton and MtCK within mitochondrial interactosome, Biochim. Biophys. Acta 1818 (2012) 1545–1554.
[52] J. Wolff, Plasma membrane tubulin, Biochim. Biophys. Acta 1788 (2009) 1415–1433.
[53] J. Cassereau, A. Chevrollier, N. Gueguen, V. Desquiret, C. Verny, G. Nicolas, F. Dubas, P. Amati-Bonneau, P. Reynier, D. Bonneau, V. Procaccio, Mitochondrial dysfunction and pathophysiology of Charcot-Marie-Tooth disease involving GDAP1 mutations, Exp. Neurol. 227 (1) (2011) 31–41.
[54] T. Narishige, K.L. Blade, Y. Ishibashi, T. Nagai, M. Hamawaki, D.R. Menick, D. Kuppuswamy, G.t. Cooper, Cardiac hypertrophic and developmental regulation of the beta-tubulin multigene family, J. Biol. Chem. 274 (1999) 9692–9697.
[55] M. Hallman, P. Maenpaa, I. Hassinen, Levels of cytochromes in heart, liver, kidney and brain in the developing rat, Experientia 28 (1972) 1408–1410.
[56] V.L. Kinnula, I. Hassinen, Effect of hypoxia on mitochondrial mass and cytochrome concentrations in rat heart and liver during postnatal development, Acta Physiol. Scand. 99 (1977) 462–466.
[57] J.J. Lehman, P.M. Barger, A. Kovacs, J.E. Saffitz, D.M. Medeiros, D.P. Kelly, Peroxisome proliferator-activated receptor gamma coactivator-1 promotes cardiac mitochondrial biogenesis, J. Clin. Invest. 106 (2000) 847–856.
[58] B.N. Finck, The PPAR regulatory system in cardiac physiology and disease, Cardiovasc. Res. 73 (2007) 269–277.
[59] Z. Wu, P. Puigserver, U. Andersson, C. Zhang, G. Adelmant, V. Mootha, A. Troy, S. Cinti, B. Lowell, R.C. Scarpulla, B.M. Spiegelman, Mechanisms controlling mitochondrial biogenesis and respiration through the thermogenic coactivator PGC-1, Cell 98 (1999) 115–124.
[60] L.K. Russell, C.M. Mansfield, J.J. Lehman, A. Kovacs, M. Courtois, J.E. Saffitz, D.M. Medeiros, M.L. Valencik, J.A. McDonald, D.P. Kelly, Cardiac-specific induction of the transcriptional coactivator peroxisome proliferator-activated receptor gamma coactivator-1alpha promotes mitochondrial biogenesis and reversible cardiomyopathy in a developmental stage-dependent manner, Circ. Res. 94 (2004) 525–533.
[61] G. Lenaz, M.L. Genova, Structural and functional organization of the mitochondrial respiratory chain: a dynamic super-assembly, Int. J. Biochem. Cell Biol. 41 (2009) 1750–1772.
[62] E. Bonora, A.M. Porcelli, G. Gasparre, A. Biondi, A. Ghelli, V. Carelli, A. Baracca, G. Tallini, A. Martinuzzi, G. Lenaz, M. Rugolo, G. Romeo, Defective oxidative phosphorylation in thyroid oncocytic carcinoma is associated with pathogenic mitochondrial DNA mutations affecting complexes I and III, Cancer Res. 66 (2006) 6087–6096.
[63] H.Y. Lim, Q.S. Ho, J. Low, M. Choolani, K.P. Wong, Respiratory competent mitochondria in human ovarian and peritoneal cancer, Mitochondrion 11 (2011) 437–443.
[64] M. Puurand, N. Peet, A. Piirsoo, M. Peetsalu, J. Soplepmann, M. Sirotkina, A. Peetsalu, A. Hemminki, E. Seppet, Deficiency of the complex I of the mitochondrial respiratory chain but improved adenylate control over succinate-dependent respiration are human gastric cancer-specific phenomena, Mol. Cell. Biochem. 370 (2012) 69–78.
[65] H. Simonnet, J. Demont, K. Pfeiffer, L. Guenaneche, R. Bouvier, U. Brandt, H. Schagger, C. Godinot, Mitochondrial complex I is deficient in renal oncocytomas, Carcinogenesis 24 (2003) 1461–1466.
[66] R.J. Scheubel, M. Tostlebe, A. Simm, S. Rohrbach, R. Prondzinsky, F.N. Gellerich, R.E. Silber, J. Holtz, Dysfunction of mitochondrial respiratory chain complex I in human failing myocardium is not due to disturbed mitochondrial gene expression, J. Am. Coll. Cardiol. 40 (2002) 2174–2181.
[67] S. Papa, The NDUFS4 nuclear gene of complex I of mitochondria and the cAMP cascade, Biochim. Biophys. Acta 1555 (2002) 147–153.
[68] J. Marin-Garcia, Thyroid hormone and myocardial mitochondrial biogenesis, Vascul. Pharmacol. 52 (2010) 120–130.
[69] P.P. Dzeja, A. Terzic, Phosphotransfer networks and cellular energetics, J. Exp. Biol. 206 (2003) 2039–2047.
[70] W.E. Jacobus, V.A. Saks, Creatine kinase of heart mitochondria: changes in its kinetic properties induced by coupling to oxidative phosphorylation, Arch. Biochem. Biophys. 219 (1982) 167–178.
[71] K. Anflous, D.D. Armstrong, W.J. Craigen, Altered mitochondrial sensitivity for ADP and maintenance of creatine-stimulated respiration in oxidative striated muscles from VDAC1-deficient mice, J. Biol. Chem. 276 (2001) 1954–1960.
[72] X. Xu, W. Decker, M.J. Sampson, W.J. Craigen, M. Colombini, Mouse VDAC isoforms expressed in yeast: channel properties and their roles in mitochondrial outer membrane permeability, J. Membr. Biol. 170 (1999) 89–102.
[73] S. Das, R. Wong, N. Rajapakse, E. Murphy, C. Steenbergen, Glycogen synthase kinase 3 inhibition slows mitochondrial adenine nucleotide transport and regulates voltage-dependent anion channel phosphorylation, Circ. Res. 103 (2008) 983–991.
[74] M. Roosimaa, T. Podramagi, L. Kadaja, A. Ruusalepp, K. Paju, R. Puhke, M. Eimre, E. Orlova, A. Piirsoo, N. Peet, F.N. Gellerich, E. Seppet, Dilation of human atria: increased diffusion restrictions for ADP, overexpression of hexokinase 2 and its coupling to oxidative phosphorylation in cardiomyocytes, Mitochondrion 13 (2013) 399–409.
[75] H. Sato, T. Nagai, D. Kuppuswamy, T. Narishige, M. Koide, D.R. Menick, G.t. Cooper, Microtubule stabilization in pressure overload cardiac hypertrophy, J. Cell Biol. 139 (1997) 963–973.
[76] E.K. Seppet, M. Eimre, T. Anmann, E. Seppet, A. Piirsoo, N. Peet, K. Paju, R. Guzun, N. Beraud, S. Pelloux, Y. Tourneur, A.V. Kuznetsov, T. Kaambre, P. Sikk, V.A. Saks, Structure–function relationships in the regulation of energy transfer between mitochondria and ATPases in cardiac cells, Exp. Clin. Cardiol. 11 (2006) 189–194.